ADAPTIVE INTENSITY MATCHING FILTERS : A NEW TOOL FOR MULTI-RESOLUTION DATA FUSION.

S. de Béthune
F. Muller
M. Binard
Laboratory SURFACES University of Liège
7, place du 20 août
B 4000 Liège, BE

1. SUMMARY

Many different multiresolution fusion methods have been proposed in the literature. An important actual aim in this field of research is to produce colour composites of multiresolution data preserving both the essential spatial information of the high resolution image and the spectral information content of the low resolution channels, so as to produce pseudo high resolution spectral channels which can be further processed for improved classification or other information extraction purposes.

The best integration results in this regard have been obtained by the HPF algorithm and by a new fusion method based on multiresolution analysis of the images using the wavelet transform.

A new methodology based on adaptive intensity matching filters using local image statistics to spectrally adjust high resolution images to the radiometry of low resolution channels is described in this paper. The algorithm tends to equalise the mean (LMM algorithm) or the mean and the variance (LMVM algorithm) of the high resolution image with those of the low resolution channels, on a pixel by pixel basis, from the values measured within a local window around each pixel position.

The INR (Intensity Normalised Ratio) transform, as defined in this paper, is a fast alternative to the RGB-IHS-RGB transform, and allows an efficient implementation of the intensity matching fusion method, generalised to images with more than three channels.

These algorithms are applied to a 1024 x 1024 window extract of a high resolution (5m) KOSMOS KVR 1000 panchromatic image to be fused with a registered low resolution (20 m) SPOT XS image, obtained over the city of Liège (Belgium).

The results obtained for varying filtering window sizes are compared with the HPF filter and the wavelet transform applied to the same set of images.

2. INTRODUCTION

The terms «fusion», «integration», «merging», «bandsharpening» have been used interchangeably in the scientific remote sensing literature to describe processes aiming at condensing information coming from multisource and multitemporal satellite image data. More specifically, these processes aim at producing colour composites preserving in the best possible way most of the significant or desired information contained in the separate images or image channels. Clearly, a choice as to which information will be relevant of the final product has to be made.

In this regard, an important effort was realised in recent years in order to preserve the highest possible spatial resolution of the available data sets without destroying spectral information content. The most usual situation in this field is the integration of three spectral channels with an high spatial resolution image.

The onset of this type of research started as soon as multisource data with different spatial resolutions became available. The best known examples concern the merging of SPOT Panchromatic images with LANDSAT TM or SPOT XS channels. These first methods applied simple arithmetic operations between channels or used principal component analysis (PCA) to condense information ([1], [2], [3], [4]). The final products correspond in general to high spatial resolution images, but with important alteration of the spectral information content of the original channels [2].

A first step toward effective spectral information conservation was introduced with the RGB-IHS-RGB transform ([5], [6], [7]). This transform is performed in three steps : (1) transform three low resolution multispectral channels from RGB to IHS space ; (2) replace the intensity channel with the high resolution channel ; and (3) perform a backward projection from IHS to RGB space. The method preserves two of the essential characteristics of the spectral colour, namely the original hue and saturation of the three spectral channels. The quality of the final product however depends on the actual differences between the original intensity channel and the intensity of the high spatial resolution image. Similar hues with identical saturation values are still strongly affected by important differences in intensity values, and are therefore not always similar looking on the final colour composite. The method performs best if there is an evident correlation between the IHS intensity component and the high resolution channel, ensuring that bright objects on the original image remain bright in the merged product [7]. Unfortunately, high correlation has no reason to be expected in most situations, where the images to be fused stem from different sensors and have been obtained at different times.

To overcome this lack of correlation between high and low resolution channels, a simple integration method consists in adding the result of a high pass filter (HPF) of the high resolution channel to the spectral channels, as was already proposed by Showengerdt [8]. This high pass filter is directly related to the structural information content of the high resolution image and removes most of its spectral information. It has a zero mean value and can be integrated in the low resolution spectral channels by calculating appropriate weighted sums, so as to ensure minimum modification of the low resolution spectral channels ([8], [9]). Chavez *et al.* [2] showed that the results generated with the HPF method are less distorted than those obtained by the traditional IHS or PCA methods.

The same approach - injecting high spatial information into the low resolution spectral channels - has also been proposed by Ranchin [10] and others ([11], [12]), and has been developed by means of multiresolution analysis of remotely sensed images using the wavelet transform [13]. Undoubtedly this approach produces the best results in regard of preservation of spectral information content of the low resolution multispectral channels [14].

This paper proposes a different approach, pursuing the same goals and achieving similar results as the multiresolution wavelet transform, and is based on adaptive intensity matching techniques using local image statistics.
In the following we shall briefly describe the wavelet merging method principle before introducing the adaptive intensity matching approach. These two methods and the HPF method will next be compared as applied to the same set of multitemporal and multiresolution data.

3. DATA FUSION BY MULTIRESOLUTION ANALYSIS AND WAVELET TRANSFORM.

This first method, called the ARSIS method (Augmentation de la Résolution Spatiale par Injection des Structures) as described by Ranchin *et al.* [14], aims at injecting high spatial structural information from the high resolution image into the low resolution channel.

The multiresolution analysis by means of the wavelet transform used to perform this task is essentially a four stage process (see figure 1, adapted from Garguet-Duport *et al.* [11] : (1) histogram matching of the high resolution image to the corresponding low resolution channel in order to adjust radiometry and improve the initial correlation between the two images. (2) perform a forward wavelet transform of the high resolution channel so as to produce four new images at the same resolution as the low resolution image. Three of these images contain the structural information of the high resolution image to be injected into the low resolution channel. They are coded by the wavelet coefficients and correspond to directional high pass filters. The fourth image, a low pass filter, corresponds to the resampled high resolution image at the resolution of the low resolution channel. (3) registering the low resolution image to the same system of reference as the high resolution image. And (4), apply the inverse wavelet transform to the registered low resolution channel, to produce a pseudo high resolution spectral channel with the added structural information content.

In order to produce a spatially enhanced colour composite, this process is successively applied to the three separate spectral channels to be combined.

4. DATA FUSION BY ADAPTIVE INTENSITY MATCHING FILTERS

As mentioned above, the quality of spectral colour preservation with the IHS transform depends on the difference between the IHS intensity channel and the high resolution channel. High correlation between these two channels will usually produce good results [7]. If, as in most instances, correlation is poor, then the only remaining alternative is to minimise the difference between the high resolution channel and the IHS intensity channel. More precisely, the original spectral information of the low resolution channels will be better preserved if the high resolution channel is made to resemble the IHS intensity channel.

Image resemblance can be achieved by matching the histograms of the two images, and is used for instance, to minimise radiometric contrast between neighbouring images in a mosaic [15]. Another approach, also producing similar histograms, is to use normalisation functions [16], which tend to equalise the means or the means and variances of the two images. Experience shows however that these approaches are strongly case dependant and that they provide the best results when the initial image correlation is high. This is because histogram matching algorithms only remodel the image frequency distribution without any control on the actual spatial distribution of the intensity values within the images.

In order to ensure true intensity matching of the images spatially, one has to be able to control and remodel the frequency distributions at a local scale. This can be performed by using adaptive filtering techniques, which have also widely been used in other domains, such as speckle removal from radar images ([17], [18]) or for image reconstruction purposes of lost data [19].

Following this approach, two local intensity matching filters, have been devised, based on the normalisation functions of Joly [16], one adjusting the local means of the images (LMM) and one adjusting both local means and variances (LMVM). The general Local Mean Matching and Local Mean Variance Matching algorithms to integrate two images, a high resolution image (H) into a low

resolution channel (L) resampled to the same size as H, are given by :

- **the LMM algorithm**

$$F_{H>L(l,c)} = \frac{DN_{H(l,c)} * M_{L(l,c)}}{M_{H(l,c)}} \quad \textbf{(1)}$$

- **the LMVM algorithm**

$$F_{H>L(l,c)} = \frac{(DN_{H(l,c)} - M_{H(l,c)})(\sigma_{L(l,c)})}{\sigma_{H(l,c)}} + M_{L(l,c)} \quad \textbf{(2)}$$

where M corresponds to the local means of the images :

$$M_{\mathrm{Im}(l,c)} = \frac{\sum_{k=c-w/2}^{c+w/2} \sum_{j=l-h/2}^{l+h/2} DN_{\mathrm{Im}(k,j)}}{hw} \quad \textbf{(3)}$$

and σ to their local standard deviations :

$$\sigma_{\mathrm{Im}(l,c)} = \frac{\sqrt{hw\left(\sum_{k=c-w/2}^{c+w/2} \sum_{j=l-h/2}^{l+h/2} DN^2_{\mathrm{Im}(k,j)}\right) - \left(\sum_{k=c-w/2}^{c+w/2} \sum_{j=l-h/2}^{l+h/2} DN_{\mathrm{Im}(k,j)}\right)^2}}{hw} \quad \textbf{(4)}$$

measured within a window of size h*w centred on the image pixel at co-ordinates (l,c), DN corresponding to the pixel values of the images.

These algorithms will produce a simulated high spatial resolution image (F) pertaining the spectral characteristics of the low resolution channel (L). How well the spectral values are preserved will depend on the size of the filtering window. Small window sizes produce the least distortion. Larger filtering windows incorporate more structural information from the high resolution image, but with more distortion of the spectral values.

If the spatial resolution ratio between the two images is important, then the pixel values of the resampled low resolution image will already correspond to a local average value of the image. Hence, in this case, the LMM algorithm (1) can be rewritten as :

$$F_{H>L(l,c)} \approx \frac{DN_{H(l,c)} * DN_{L(l,c)}}{M_{H(l,c)}} \quad \textbf{(5)}$$

which shows that the LMM filtered image corresponds to the low resolution channel multiplied by the image_to_local_mean ratio of the high resolution image.

The LMVM algorithm becomes :

$$F_{H>L(l,c)} \approx \frac{(DN_{H(l,c)} - M_{H(l,c)})\sigma_{L(l,c)}}{\sigma_{H(l,c)}} + DN_{L(l,c)} \quad \textbf{(6)}$$

The resampling process of the low resolution image to the same scale as the high resolution image drastically reduces its local standard deviations ($\sigma_{L(l,c)} \approx 0$), especially if the resolution ratio between the images is high and for small filtering window sizes. In this instance, equation (6) simply reduces to the limiting case :

$$F_{H>L(l,c)} \approx DN_{L(l,c)} \quad \textbf{(7)}$$

The fused image will not significantly differ from the low resolution image. In this case, larger local environments should be taken to perform the filtering in order to incorporate more information from the high resolution image.

Without the constraint of variance equalisation, equation **(6)** becomes :

$$F_{H>L(l,c)} \approx DN_{H(l,c)} - M_{H(l,c)} + DN_{L(l,c)} \quad \textbf{(8)}$$

and corresponds to the HPF integration filter defined by Showengerdt [8]. This formulation also corresponds to the additive form of equation **(5)**.

4.1. Procedural steps for implementing image fusion by adaptive intensity matching.

As described earlier, the LMM and LMVM filters perform an intensity matching of two channels which have previously been registered. Hence, this process can be applied between the high resolution channel and three individual low resolution spectral channels producing three spatially enhanced images which can then be combined to form the desired colour composite.

Instead of applying the filtering algorithms to each of the separate channels, a simplified method can be adopted based on the IHS conversion. If three channels have to be merged with a high spatial resolution image, these channels can first be converted from RGB to IHS space. The high resolution image will then be intensity matched to the IHS intensity channel and substituted to this channel before a reverse projection back into RGB space. The resulting RGB channels correspond to the spatially enhanced spectral channels, and are obtained after only one filtering process.

4.2. Generalising the data fusion implementation with the INR transform

An improvement of this implementation method, leading to a further simplification and a generalisation of the procedure to more than three channels, has been devised. It is based on a new analytic formulation of IHS space.

When an IHS-RGB transform is performed, only the intensity channel is taken into account and replaced, while the hue and the saturation channels are left unchanged. It is however necessary to compute both these channels as they are needed in the reverse conversion from IHS to RGB space.

The relationships between RGB and IHS space are presented on figure 2.

The RGB axes of the RGB cube correspond to an hypothetical SPOT multispectral image (XS3, XS2 and XS1 channels). Crosscutting the RGB cube, the IHS space is schematically represented by the RGB triangle, perpendicular to the Intensity (I) axis, which can be defined as the sum of the three XS channels ([5], [20], [21]) :

$$I = XS1 + XS2 + XS3 \qquad \textbf{(9)}$$

The triangle itself corresponds to the two dimensional Hue-Saturation plane. The expressions of the Hue and Saturation co-ordinates are cyclic, and depend on the position of the individual colours inside the three subtriangles making up the RGB triangle [5]. We can express Hue on a scale ranging from 0 (= blue) to 3 (= 0 = blue) where the particular values 1 and 2 correspond respectively to green and red hues. Saturation can be expressed on a scale of 0 (= no saturation) to 1 (= total saturation). For each subtriangle we thus have :

$$\begin{aligned} H_1 &= (XS2 - XS3)/(I - 3XS3) \\ H_2 &= 1 + (XS3 - XS1)/(I - 3XS1) \\ H_3 &= 2 + (XS1 - XS2)/(I - 3XS2) \end{aligned} \qquad \textbf{(10)}$$

$$\begin{aligned} S_1 &= (I - 3XS3)/(I - 2XS3) \\ S_2 &= (I - 3XS1)/(I - 2XS1) \\ S_3 &= (I - 3XS2)/(I - 2XS2) \end{aligned} \qquad \textbf{(11)}$$

where the subscripts refer to the particular subtriangles illustrated on figure 2.

Individual colours plotted onto the RGB plane by projection from the origin (O) of the axes can also be described in terms of the normalised ratios of the three colour components (barycentric co-ordinates) as shown on figure 2. Hence, description of IHS space can advantageously be replaced by what we shall define as INR space, standing for Intensity-Normalised Ratio space. Three co-ordinates are necessary to define this space, the usual intensity co-ordinate and two normalised ratios :

$$\begin{aligned} I &= XS1 + XS2 + XS3 \\ XS1_N &= XS1 / I \\ XS2_N &= XS2 / I \end{aligned} \qquad \textbf{(12)}$$

The third normalised ratio is redundant as it can be deduced from the first two:

$$XS3_N = XS3 / I = 1 - XS1_N - XS2_N \qquad \textbf{(13)}$$

Performing a backward transformation of IHS to RGB space with preservation of hue and saturation, amounts to say that the normalised ratios of the three channels are also preserved. Hence, if a panchromatic SPOT image (PAN) has been substituted to the IHS intensity channel, then the backward transform should produce three new channels for which the following relations hold :

$$I_{new} = PAN = XS1_{new} + XS2_{new} + XS3_{new} \qquad \textbf{(14)}$$

and

$$\begin{aligned} XS1_{new} / PAN &= XS1_N = XS1 / I \\ XS2_{new} / PAN &= XS2_N = XS2 / I \\ XS3_{new} / PAN &= XS3_N = XS3 / I \end{aligned} \qquad \textbf{(15)}$$

Rewriting these equations yields :

$$\begin{aligned} XS1_{new} &= XS1 * PAN / I \\ XS2_{new} &= XS2 * PAN / I \\ XS3_{new} &= XS3 * PAN / I \end{aligned} \qquad \textbf{(16)}$$

showing that a data integration procedure by INR transform only requires computation of the global intensity channel of the three low resolution multispectral channels even without having to compute any normalised ratio beforehand. These relations also clearly stress the fact that the original channel ratios are preserved by the new multispectral channels. The new channels are of course identical to those obtained by a classic RGB-IHS-RGB transform.

Furthermore the data fusion by INR transform is easily generalised for multispectral data of more than three channels, such as for instance LANDSAT TM multispectral images. For n channels (ch) to be upgraded with a high resolution image (H) we thus have :

$$I = \sum_{i=1}^{n} ch_i \qquad \textbf{(17)}$$

$$new\_ch_i = ch_i * H / I \qquad \textbf{(18)}$$

By this method, only one intensity matching filtering of the high resolution image to the global intensity channel is needed to produce all the integrated upgraded spectral channels.

Based on this approach, the general merging method can be described in four steps as illustrated on figure 3.
The first step is to register the low resolution multispectral channels to the high resolution image (H), so as to obtain resampled multispectral channels (r) overlaying exactly the high resolution image. This increases artificially the spatial resolution of the channels, as their pixel size diminishes, but without increasing their spatial information content, so that they still have to be considered as low resolution channels. These channels are then summed up (step 2) to produce a low resolution global intensity channel (L) to which the high resolution image (H) will be intensity-matched (step 3), resulting in a high resolution global intensity matched image (F). The

final step applies the INR transform to the low resolution resampled channels (ri) using the F and L images, yielding the simulated high resolution multispectral channels.

5. DATA DESCRIPTION AND APPLICATION

The three fusion algorithms (LMVM, LMM and HPF) were applied with different window sizes to a SPOT XS scene to be integrated with a panchromatic KOSMOS KVR 1000 image, and the results are compared with those obtained by the ARSIS method computed by Dr. T. Ranchin at the University of Sophia-Antipolis (Nice, France).

The two images were taken above the city of Liège (Belgium), respectively in May and in June of 1992. The KOSMOS image, with a nominal resolution of two meters was registered to the 1:25000 topographic basemap and resampled by cubic convolution to 5 meters, in order to reduce the original resolution ratio between the two sets of data from 10 to 4. The three SPOT XS channels were then registered to the KOSMOS image, and also resampled by cubic convolution to 5 meter pixels. A square window extract of 1024 x 1024 pixels over the south-eastern part of the city was selected to perform the integration analysis (figure 4.).

This study area along the Meuse river is characterised by recent industrial development and suburban growth. Figure 4 shows the river harbour bordered by industrial zonings to the south and to the east, urban and suburban areas to the north-west and mixed forest and agricultural areas to the south-east.

Table 1 summarises the main statistical characteristics of the three SPOT XS channels and of the KOSMOS image. The XSI channel corresponds to the intensity channel of the IHS transform. The entropy value is a measure of the average amount of information of the channel, as described by different authors ([22],[23]) :

$$Entropy = \sum_{i=0}^{255} - p_i * \log_2(p_i) \quad \textbf{(19)}$$

where p_i is the probability of level i in the image.

As can be seen in table 1, the KOSMOS image is characterised by much higher standard deviation and entropy values than the corresponding SPOT XS channels.

Table 1 : Image statistics and spatial resolution

	Mean	Median	St. Dev.	Entropy	Range
KVR	137.72	139.5	56.29	7.6400	236
XS1	53.89	53.5	6.58	4.5555	100
XS2	43.14	42.5	8.76	4.9804	120
XS3	63.12	60.5	20.36	6.2546	157
XSI	53.05	52.5	8.32	4.9076	123

Table 2 presents the correlation between the different channels. The correlation between the two channels in the visible part of the spectrum (XS1, XS2) is elevated, but is low between the visible and infrared part (XS3) of the spectrum. Although the two images were taken at only two months interval, the KOSMOS image does not really correlate well with any of the XS channels. The quite low KVR-XSI correlation value precludes a satisfactory fusion between these images by the traditional IHS method, as it will significantly distort the spectral values of the original low resolution channels [7].

Table 2 : Correlation between the different image channels

	KVR	XS1	XS2	XS3	XSI
KVR	1.000				
XS1	0.6240	1.000			
XS2	0.6210	0.9611	1.000		
XS3	-0.0428	-0.0306	-0.0398	1.000	
XSI	0.3474	0.5756	0.5714	0.7934	1.000

The three LMVM, LMM and HPF merging algorithms were applied to this set of images with 6 different window sizes, ranging from 3 x 3 to 49 x 49 pixels in size. In order to assess the quality of the different fusion algorithms applied to the images, a set of statistical parameters based on the criteria proposed by Ranchin *et al.* [14] were computed (tables 3 to 5) and are illustrated on figure 5., together with the same data corresponding to the original images and those obtained by the ARSIS method. Ideally, the mean and the standard deviation of the integrated and of the original channels should remain as close as possible. Similarly, correlation between these channels shoud be as near as possible to one [14].

These tables also lists the entropies of the different results, allowing to analyse the added information content of the integrated channel as compared to the original channel. The last parameter listed in these tables is a deviation index (d_index) as defined by Costantini *et al.* [24] :

$$d\_index = \frac{1}{lc} \sum_{i=1}^{l} \sum_{j=1}^{c} \frac{\left| F_{i,j} - L_{i,j} \right|}{L_{i,j}} \quad \textbf{(20)}$$

which measures de relative deviation of the fused image (F) of that of the original low resolution reference channel (L). The smaller this value, the better the image quality.

5.1 The LMVM filter (table 3 ; figure 5)

By construction, the mean and standard deviation of the fused images remain constant for all filtering window sizes. Entropy remains constant for small window sizes (3 to 7). Correlation values also remain practically constant, very near the maximum possible value. At these local scales the differences between the reference image and the fused images are so small that they do not bear any real significance. This is due to the fact that, at

these scales, the local variance values of the resampled reference image (L) are nearly zero because of the quite high resolution ratio between the two images, so that equation (6) simply reduces to the limiting case of equation (7).

With increasing window size (from 15 to 49), entropy, correlation and deviation index start changing significantly. Entropy and deviation index gradually increase with window size, whereas correlation values decrease. Referring to the numbers, the closest match to the ARSIS filtered image is the Local Mean Variance Matched image with a window size of 15, although bigger window sizes also produce good results with still quite high correlation values (0.8 for window size 49). Visually, the fused images obtained with large window sizes (from 15 to 49) remain very close to the ARSIS filtered image.

5.2. The LMM filter (table 4, figure 5)

Here too, by construction, the mean of the fused images remains practically constant for all filtering window sizes. Standard deviation, entropy and deviation index increase
steadily with filter window size, while correlation decreases continuously. Comparing the numbers, the ARSIS filtered image lies somewhere in between the LMM3 and LMM5 filtered images. Visually, for these small window sizes, the LMM algorithm produces images the most similar to the ARSIS image.

5.3. The HPF filter (table 5, figure 5)

The HPF filter, introduced by Showngerdt [9], simply adds a high pass filter of the high resolution image to the resampled low resolution channel. The high pass filter has a mean value of zero and therefore preserves the mean of the filtered images for all filtering window sizes. Standard deviation, entropy and deviation index increase rapidly with filtering window size, while correlation diminishes very fast. Although considered one of the best integration methods so far [7], it does not compare favourably with the three other integration methods described, producing images with more distorted spectral values.

6. CONCLUSIONS

This study has shown that data integration of a high spatial resolution image into low spatial resolution channels of a multispectral image can conveniently be performed by mean of intensity matching the high resolution image with the low resolution channels. This intensity matching is performed by locally adjusting the mean (LMM) or the mean and variance (LMVM) of the high resolution image to that of the low resolution channels.

The spectral values of the original low resolution channels are the best preserved when filtering the images with the smallest possible window sizes. In

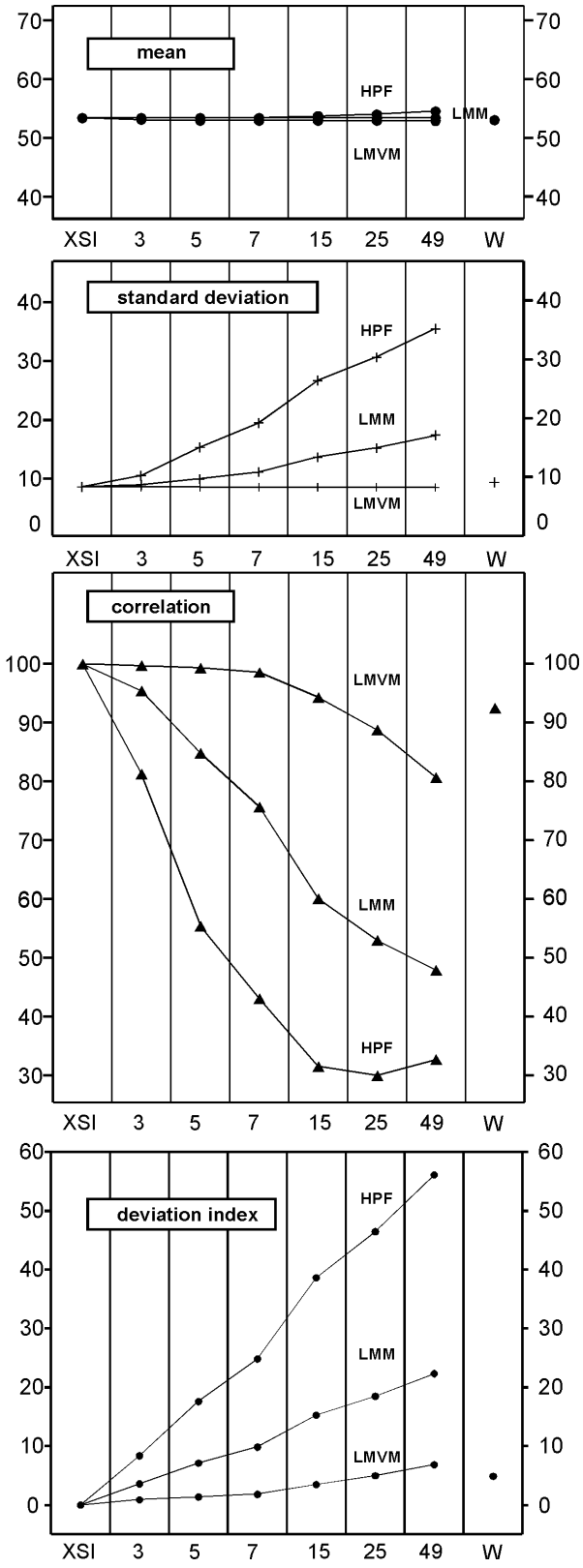

Figure 5
LMVM, LMM and HPF filtered image statistics in function of filtering window size. XSI is the reference image. W is the image filtered by the ARSIS method.

the case of the LMM algorithm, window sizes of 3 to 5 produce the results which compare best with

the image produced by the ARSIS method. In the case of the LMVM algorithm, the smallest filtering window sizes produce no significant difference between the original channel and the fused image. Only with bigger window sizes does the information content of the fused image start to increase significantly while still preserving the spectral characteristics of the original channels.

AKNOWLEDGEMENTS

This research was partially conducted within the framework of a cooperative pilot research project on feature extraction from high spatial resolution satellite imagery and a joint Sino-Belgian research project on spatiomapping funded by the Belgian OSTC (contracts n° T3/12/47 and IN-CH 005). The authors wish to thank Dr. T. Ranchin for providing the integrated image with the ARSIS method as also for his helpful suggestions and comments.

REFERENCES

[1] Chavez, P.S. Jr., (1986), Digital merging of Landsat TM and digitised NHAP data for 1: 24,000 scale image mapping, Photogrammetric Engineering and Remote Sensing, 52, 10, pp.1637-1646.

[2] Chavez, P.S. Jr., Sides, S.C. and Anderson, J.A., (1991), Comparison of three different methods to merge multiresolution and multispectral data: Landsat TM and SPOT Panchromatic, Photogrammetric Engineering & Remote Sensing, 57, 3, pp. 295-303.

[3] Cliche, G., Bonn, F. , Teillet, P., (1985), Integration of the SPOT panchromatic channel into its multispectral mode for image sharpness enhancement, Photogrammetric Engineering and Remote Sensing, 51, 3, pp. 311-316.

[4] Welch, R. and Ehlers, M., (1987), Merging Multiresolution SPOT HRV and Landsat TM data, Photogrammetric Engineering and Remote Sensing, 53, 3, pp. 301-303.

[5] Sabins, F.F. Jr., (1987), Remote Sensing. Principles and Interpretation. 2e ed.,Freeman, New York, 449 p.

[6] Lillesand, T.M. and Kiefer, R.W., (1987), Remote Sensing and image interpretation, 2e ed., John Wiley & Sons, 721 p.

[7] Carper W.J., Lillesand T.M., Kiefer, R.W, (1990), The use of Intensity-Hue-Saturation transformations for merging SPOT Panchromatic and Multispectral Image Data, Photogrammetric Engineering and Remote Sensing, 56, 4, pp. 459-467.

[8] Showengerdt, R.A., (1980), Reconstruction of multispatial, multispectral image data using spatial frequency contents, Photogrammetric Engineering & Remote Sensing, 46, 10, pp. 1325-1334.

[9] Vrabel J., (1996), Multispectral imagery band sharpening study, Photogrammetric Engineering & Remote Sensing, 62, 9, pp. 1075-1083.

[10] Ranchin, T., (1993), Applications de la transformée en ondelettes et de l'analyse multirésolution au traitement des images de télédétection. Unpublished PhD Thesis, University of Nice-Sophia Antipolis, 146 p.

[11] Garguet-Duport, B., Girel, J., Chassery, J-M ., and Pautou, G., (1996), The use of multiresolution analysis and wavelets transform for merging SPOT panchromatic and multispectral image data, Photogrammetric Engineering & Remote Sensing, 62, 9, pp. 1057-1066.

[12] Yocky, D.A., (1996), Multiresolution wavelet decomposition image merger of Landsat thematic mapper and SPOT panchromatic data, Photogrammetric Engineering & Remote Sensing, 62, 9, pp. 1067-1074.

[13] Ranchin, T., Wald, L, (1993), The wavelet transform for the analysis of remotely sensed images. International Journal of Remote Sensing , 14, 3, pp 615-619.

[14] Ranchin, T., Wald, L., Mangolini, M. and Penicand, C., (1996), On the assessment of merging processes for the improvement of the spatial resolution of multispectral SPOT XS images. In Proceedings of the conference "Fusion of Earth data: merging point measurements, raster maps and remotely sensed images", Cannes, France, February 6-8, 1996, Thierry Ranchin and Lucien Wald Editors, published by SEE/URISCA, Nice, France, pp. 59-67.

[15] Richards, A.J.,(1986), Remote Sensing Digital Image Analysis. An Introduction., Spriger-Verlag, 281 p.

[16] Joly, G., (1986), Traitements des fichiers-images, Télédétection Satellitaire 3, Ed. Paradigme, 137 p.

[17] Frost, V.S., Styles, J.A., Shanmugan, K.S., and Holzman, J.C. , (1982), A model for radar images and its application to adaptive digital filtering of multiplicative noise, IEEE Transactions on Pattern Analysis and Machine Intelligence, PAM 1-4, pp. 157-166.

[18] Lee, J.S., 1981, Refined filtering of image noise using local statistics, Computer Graphics and Image Processing, 15, pp. 380-389.

[19] Fusco L. , Trevese D., (1985), On the reconstruction of lost data in images of more than one band., *International Journal of Remote Sensing,* 6, pp.1535-1544.

[20] Liu, J.G. and McM. Moore, J., (1990), Hue image RGB colour composition. A simple technique to suppress shadow and enhance spectral signature, International Journal of Remote Sensing, 11, 8, pp. 1521-1530.

[21] Edwards K., Davis, P.A., (1994), The use of Intensity-Hue-Saturation transformation for producing colour shaded-relief images, Photogrammetric Engineering & Remote Sensing, 60, 11, pp. 1369-1374.

[22] Moik, J., (1980), Digital processing of remotely sensed images. NASA Special Publication 431, Washington DC.

[23] Mather, P.M., (1987), Computer processing of remotely sensed images. An Introduction. John Wiley & Sons, 352 p..

[24] Costantini, M., Farina, A., Zirilli, F., (1997), The fusion of different resolution SAR images, Proceedings of the IEEE, 85, 1, pp. 139-146.

Table 3 : Local Mean Variance Matching Statistics									
window	KVR	XSI	LMVM 3	LMVM 5	LMVM 7	LMVM 15	LMVM 25	LMVM 49	ARSIS
Mean	137.72	53.39	53.39	53.40	53.40	53.40	53.41	53.40	53.05
St. Dev.	56.29	8.32	8.32	8.30	8.29	8.28	8.30	8.27	9.10
Entropy	7.6400	4.9062	4.9049	4.9033	4.9042	4.9169	4.9356	4.9371	5.1067
Correlat.	0.3474	1.0000	0.9973	0.9929	0.9858	0.9431	0.8878	0.8065	0.9253
d_index	1.5985	0.0000	0.0090	0.0137	0.0182	0.0347	0.0498	0.0685	0.0488

Table 4 : Local Mean Matching Statistics									
window	KVR	XSI	LMM 3	LMM 5	LMM 7	LMM 15	LMM 25	LMM 49	ARSIS
Mean	137.72	53.39	53.12	52.98	52.96	52.95	52.94	52.91	53.05
St. Dev.	56.29	8.32	8.67	9.70	10.81	13.38	14.97	17.04	9.10
Entropy	7.6400	4.9062	5.0397	5.2555	5.4320	5.7528	5.9133	6.0825	5.1067
Correlat.	0.3474	1.0000	0.9541	0.8484	0.7572	0.6004	0.5298	0.4787	0.9253
d_index	1.5985	0.0000	0.0358	0.0712	0.0986	0.1529	0.1848	0.2233	0.0488

Table 5 : Local High Pass Filter Statistics									
window	KVR	XSI	HPF 3	HPF 5	HPF 7	HPF 15	HPF 25	HPF 49	ARSIS
Mean	137.72	53.39	53.39	53.39	53.41	53.72	54.02	54.55	53.05
St. Dev.	56.29	8.32	10.24	15.06	19.20	26.43	30.38	35.22	9.10
Entropy	7.6400	4.9062	5.3488	5.9466	6.3097	6.7182	6.8319	6.8848	5.1067
Correlat.	0.3474	1.0000	0.8128	0.5540	0.4305	0.3152	0.2295	0.3271	0.9253
d_index	1.5985	0.0000	0.0838	0.1760	0.2483	0.3863	0.4647	0.5613	0.0488

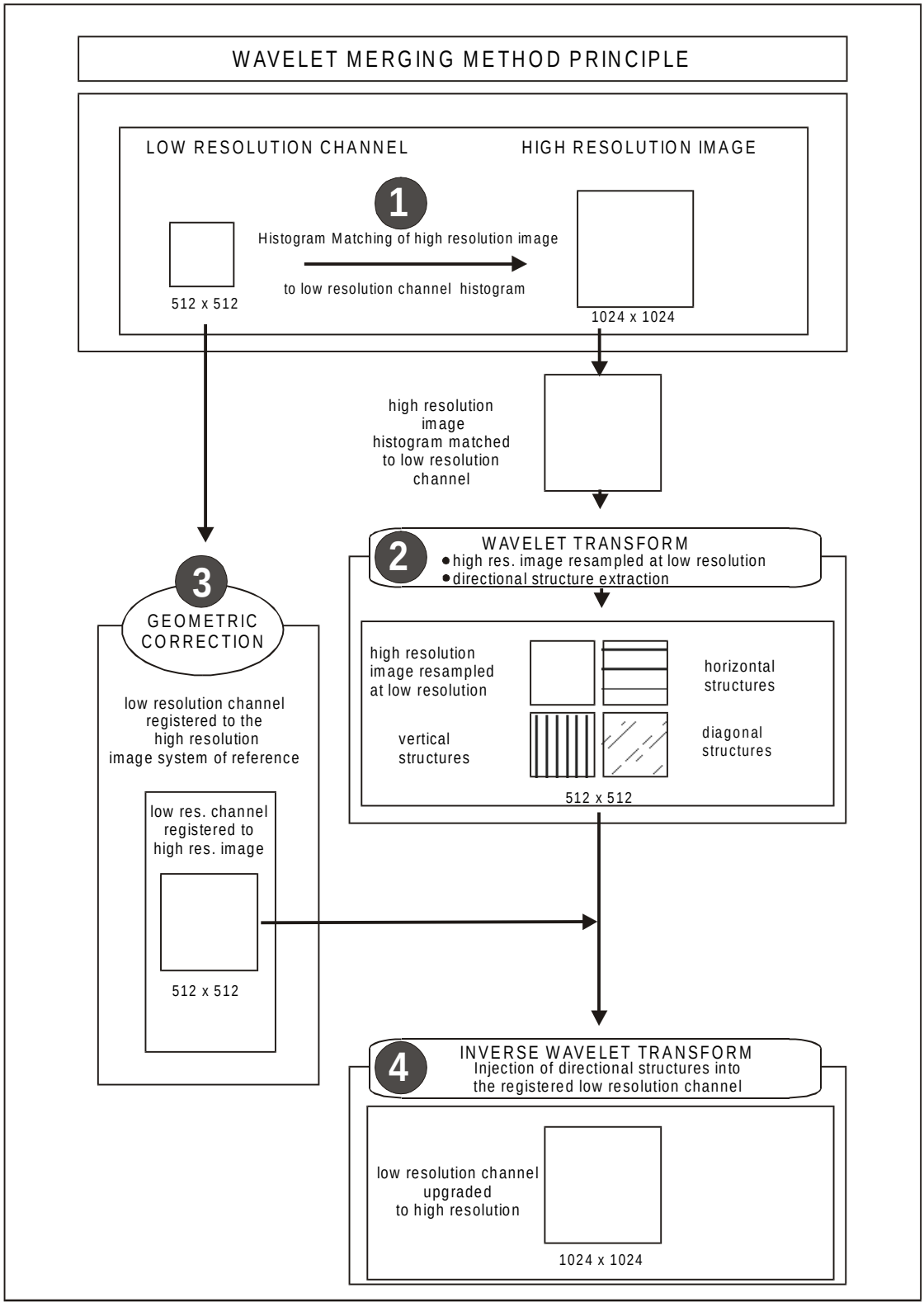
WAVELET MERGING METHOD PRINCIPLE
LOW RESOLUTION CHANNEL
HIGH RESOLUTION IMAGE
1
Histogram Matching of high resolution image
to low resolution channel histogram
512 x 512
1024 x 1024
high resolution image histogram matched to low resolution channel
2
WAVELET TRANSFORM
high res. image resampled at low resolution
directional structure extraction
high resolution image resampled at low resolution
horizontal structures
vertical structures
diagonal structures
512 x 512
3
GEOMETRIC CORRECTION
low resolution channel registered to the high resolution image system of reference
low res. channel registered to high res. image
512 x 512
4
INVERSE WAVELET TRANSFORM
Injection of directional structures into the registered low resolution channel
low resolution channel upgraded to high resolution
1024 x 1024

Figure 1

GEOMETRIC RELATIONS IN RGB-IHS SPACE

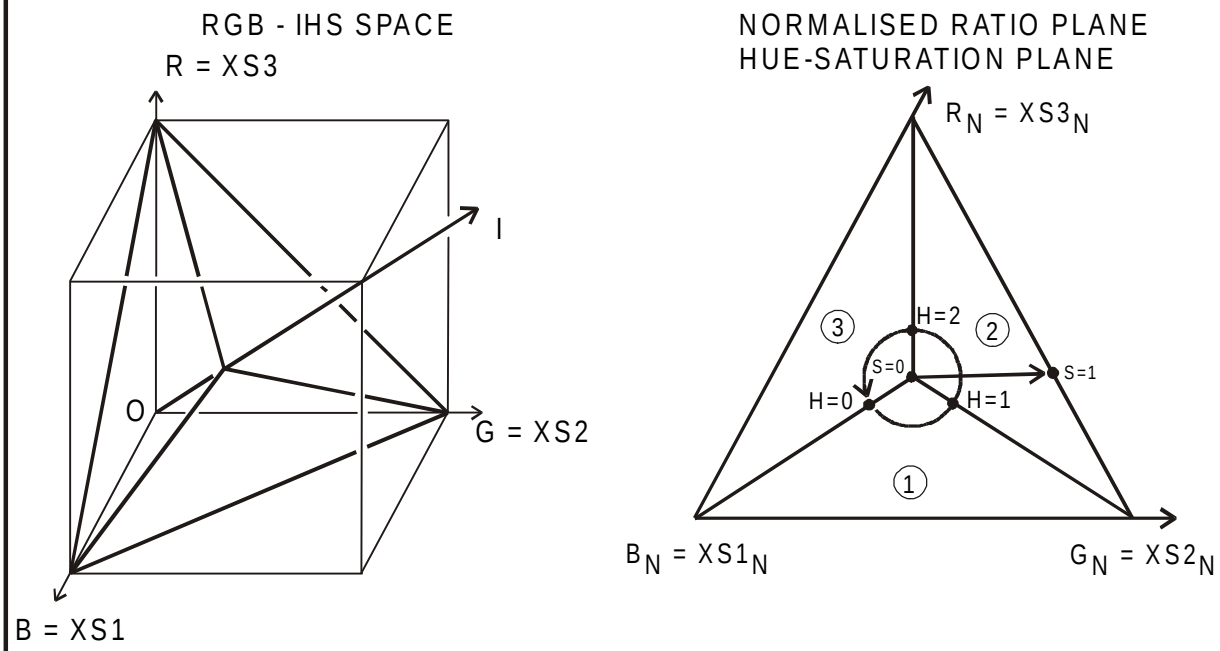

RGB coordinates	IHS coordinates	INR coordinates
R = XS3 G = XS2 B = XS1	I = XS1 + XS2 + XS3 ① H = (XS2-XS3)/(I-3XS3) C ② S = (I-3XS3)/(I-2XS3) C ③	I = XS1 + XS2 + XS3 $XS3_N = XS3/I$ $XS2_N = XS2/I$

Figure 2

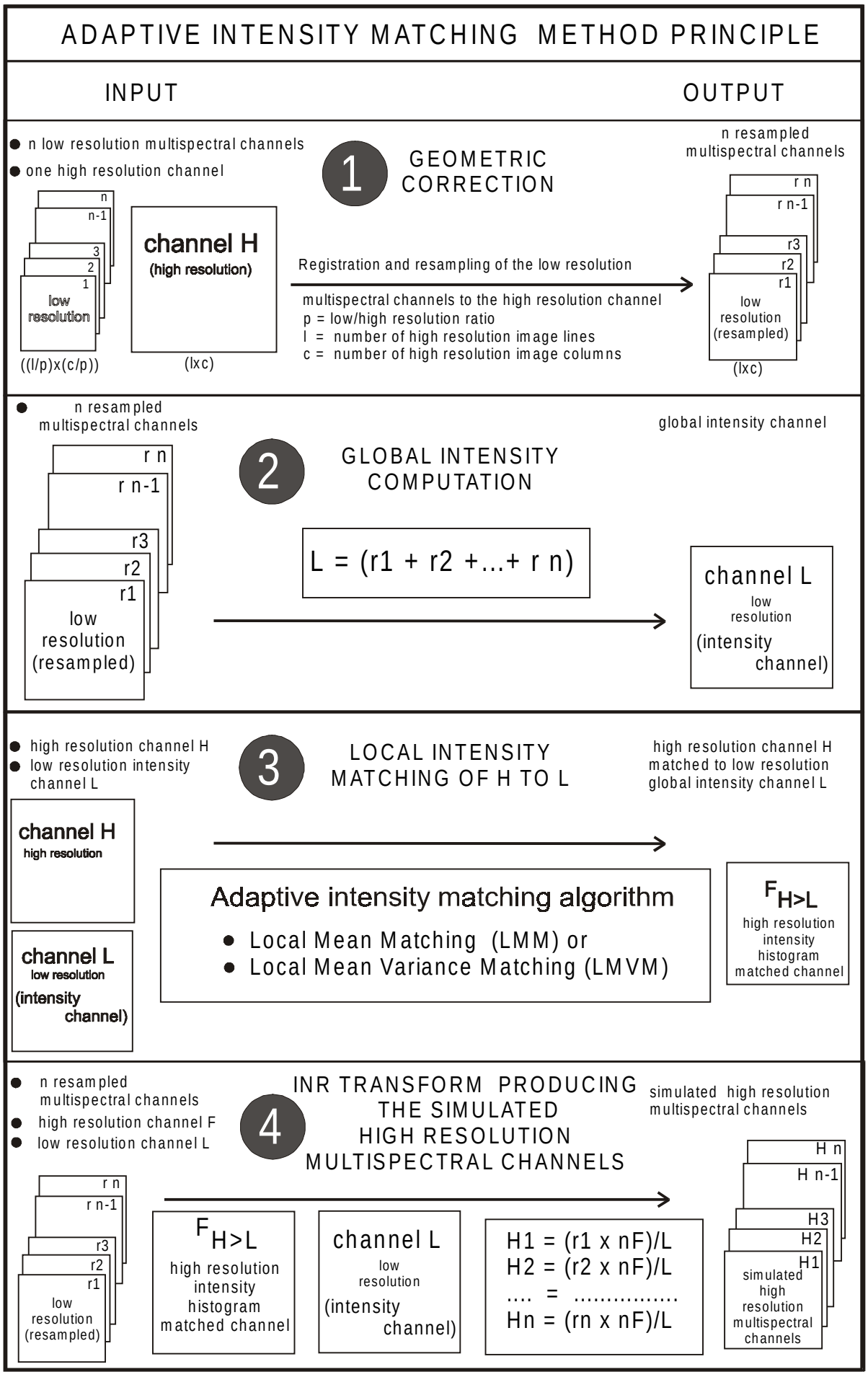
ADAPTIVE INTENSITY MATCHING METHOD PRINCIPLE
INPUT
OUTPUT
n low resolution multispectral channels
one high resolution channel
n
n-1
3
2
1
low resolution
((l/p)x(c/p))
channel H
(high resolution)
(lxc)
1
GEOMETRIC CORRECTION
Registration and resampling of the low resolution
multispectral channels to the high resolution channel
p = low/high resolution ratio
l = number of high resolution image lines
c = number of high resolution image columns
n resampled multispectral channels
r n
r n-1
r3
r2
r1
low resolution (resampled)
(lxc)
n resampled multispectral channels
r n
r n-1
r3
r2
r1
low resolution (resampled)
2
GLOBAL INTENSITY COMPUTATION
L = (r1 + r2 +...+ r n)
global intensity channel
channel L
low resolution
(intensity channel)
high resolution channel H
low resolution intensity channel L
channel H
high resolution
channel L
low resolution
(intensity channel)
3
LOCAL INTENSITY MATCHING OF H TO L
high resolution channel H matched to low resolution global intensity channel L
Adaptive intensity matching algorithm
Local Mean Matching (LMM) or
Local Mean Variance Matching (LMVM)
F H>L
high resolution intensity histogram matched channel
n resampled multispectral channels
high resolution channel F
low resolution channel L
r n
r n-1
r3
r2
r1
low resolution (resampled)
4
INR TRANSFORM PRODUCING THE SIMULATED HIGH RESOLUTION MULTISPECTRAL CHANNELS
F H>L
high resolution intensity histogram matched channel
channel L
low resolution
(intensity channel)
H1 = (r1 x nF)/L
H2 = (r2 x nF)/L
.... = ...
Hn = (rn x nF)/L
simulated high resolution multispectral channels
H n
H n-1
H3
H2
H1
simulated high resolution multispectral channels

Figure 3

KOSMOS KVR 1000 IMAGE OVER S-E OF LIEGE (BE)

resampled to 5 m resolution

1024 x 1024

Figure 4